Effects of Bamboo Fiber Substitution for Glass Fibers on Mechanical and Erosive Wear Properties of High-Density Polyethylene Composites

Qianhui Yin,[a,b] Liangpeng Jiang,[a,b,*] Zitong Wang,[a] Kaiwen Xue,[a] and Guoyan Duan [c]

To explore the feasibility of replacing inorganic fibers with plant fibers for the fabrication of polymer composites for waterfront engineering applications, the effects of replacing glass fibers with bamboo fibers on the mechanical and erosive wear properties of high-density polyethylene (HDPE) composites were investigated. Mechanical performance tests and the hydraulic abrasive erosive wear technique, which is based on a rotating jet system, were employed. The results indicated that as the mass ratio of bamboo fibers to glass fibers increases, the mechanical properties of the HDPE composites improved overall, while the erosion resistance initially decreased and then increased. The maximum increases in tensile, flexural, and impact strength, as well as breakage elongation were 16.4%, 13.8%, 34.9%, and 10.0%, respectively. Bamboo fibers, when replacing glass fibers, can form chemical bonds with the matrix, suppressing the brittle fracture characteristics observed in the tensile sections of HDPE composites. However, this substitution also reduced the erosion resistance of the HDPE composites. The wear characteristics of the eroded surfaces mainly include a brittle fracture of the matrix and fragmentation, as well as extensive exposure of the bamboo fibers.

DOI: 10.15376/biores.20.2.4033-4043

Keywords: Bamboo fibers; Glass fibers; High-density polyethylene; Composites; Mechanical properties; Erosive wear

*Contact information: a: School of Mechanical and Energy Engineering, Guangdong Ocean University, Yangjiang 529500, China; b: Anhui Intelligent Mine Technology and Equipment Engineering Laboratory, Anhui University of Science and Technology, Huainan 232001, China; c: Southeast University Chengxian College, Nanjing 210000, China; *Corresponding author: jianglp98@outlook.com*

INTRODUCTION

Polymer composites can be reinforced by either inorganic fibers or plant fibers (Kunishima *et al.* 2020; Xu *et al.* 2021). Compared with plant fibers, inorganic fibers have superior strength, rigidity, and load-bearing capacity. Polymer composites reinforced with inorganic fibers are often used in applications where they are subjected to various loading conditions, such as tension, bending, impact, and compression, as well as tribological environments where two-body and three-body frictional wear frequently occur. Therefore, scholars have long been committed to studying the mechanical and tribological properties of inorganic fiber-reinforced polymer composites (Wang *et al.* 2021; Cao *et al.* 2022).

With the global rise in carbon awareness, the mechanical and tribological properties of plant fiber-reinforced polymer (PFRP) composites have attracted increasing attention (Jenish *et al.* 2022; Rangappa *et al.* 2022; Palanisamy *et al.* 2024; Ramakrishnan *et al.* 2024). Reinforcing PFRP composites with glass fibers and inorganic nanoparticles can increase their tensile, flexural, and impact strengths, while fiber modification does not

significantly affect the tensile strength or tensile modulus of PFRP composites (Zhang *et al.* 2016; Qi *et al.* 2019; Zhang *et al.* 2020). The type of wood flour and hemp fibers significantly affect the sliding wear performance of PFRP composites, and fiber modification can improve the sliding wear resistance of these composites (Goriparthi *et al.* 2012; Jeamtrakull *et al.* 2012; Bajpai *et al.* 2013). Reinforcement with copper slag, red mud, and alumina can enhance the pneumatic abrasive erosive wear performance of PFRP composites (Das *et al.* 2017; Kalusuraman *et al.* 2019; Vigneshwaran *et al.* 2019). Most research has focused on the effects of inorganic fillers, fiber modifications, and fiber types on the mechanical and tribological properties of PFRP composites, while studies on how replacing inorganic fibers with plant fibers affects the aforementioned properties of polymer composites remain scarce. Furthermore, as novel materials for waterfront engineering (*e.g.*, harbors and wharves), PFRP composites have been widely investigated for their sliding wear and pneumatic abrasive erosive wear properties. However, their hydraulic abrasive erosive wear properties have attracted less attention (Jiang *et al.* 2022a,b; Li *et al.* 2022).

This study investigated the effects of bamboo fiber substitution for glass fibers on the mechanical and erosive wear properties of high-density polyethylene (HDPE) composites, utilizing mechanical performance tests and the hydraulic abrasive erosive wear technique, which is based on a rotating jet system. In addition, chemical structure analysis, microscopic morphology observation, and elemental distribution detection techniques were employed. The results provide theoretical foundations and technical support for the preparation of polymer composites for waterfront engineering by replacing inorganic fibers with plant fibers.

EXPERIMENTAL

Raw Materials

Bamboo fibers with a particle size of 149 μm and length/diameter (*L*/*D*) ratio of 3.5 were sourced from Mujiang Weihua Spice Factory, Jiangmen, China. Glass fibers with a particle size of 23 μm and an *L*/*D* ratio of 13.0 were sourced from Weijia Composite Materials Co., Ltd., Wuhe, China. HDPE with a melt flow index of 0.94 g/10 min was sourced from Sinopec Group Co., Ltd., Beijing, China. Maleic anhydride grafted polyethylene (MAPE) was sourced from Jinghong Polymer Materials Co., Ltd., Dongguan, China.

Specimen Preparation

The bamboo fibers, glass fibers, HDPE, and MAPE were pre-dried in an oven at 100 °C for 6 h. The pre-dried raw materials were weighed according to the specimen number and composition mass ratios presented in Table 1, and then they were subjected to mixing through ball milling. The mixed raw materials were placed in a mold for compression molding. The molding temperature, pressure, and time were 170 °C, 30 MPa, and 12 min, respectively. The process was conducted using a plate vulcanizing machine (XW-212C, Xunwei Checking & Measuring Instrument Co., Ltd., Dongguan, China). The specimens were prepared with dimensions of 100 × 100 × 5 mm^3 and were cut according to test requirements after cooling to room temperature.

Table 1. Serial Number and Mass Ratio of the Specimens

Specimen ID	Mass ratio			
	Bamboo fiber	Glass fiber	HDPE	MAPE
S1	0	80	100	2
S2	15	65	100	2
S3	30	50	100	2
S4	45	35	100	2
S5	60	20	100	2

Characterization

Mechanical properties

The tensile and flexural properties of the specimens were tested in accordance with GB/T 1040.1-2006 and GB/T 9341-2000, respectively. The tests were conducted using an universal testing machine (CTM8050, Xieqiang Instrument Manufacturing Co., Ltd., Shanghai, China). The specimen dimensions were 100 × 10 × 5 mm³, and the test speed was 2 mm/min. The test results were averaged over five repetitions.

The impact properties of the specimens were tested in accordance with ASTM D256-2010 (2018) using a pendulum impact tester (FBS-5.5DZ, Forbs Testing Equipment Co., Ltd., Xiamen, China). The specimen dimensions were 100 × 10 × 5 mm³, and the impact velocity was 3.4 m/s. The test results were averaged over five repetitions.

Composite structures

Fourier transform infrared (FTIR) spectroscopy was employed to analyze the bonding mechanisms between fibers and the matrix. This analysis was performed using a FTIR spectrometer (Nicolet iS50, Thermo Fisher Scientific, Co., Ltd., Shanghai, China). The wavenumber accuracy was better than 0.005 cm^{-1}, and the resolution was better than 0.09 cm^{-1}.

The microscopic morphology of the tensile sections was analyzed to evaluate the bonding quality between fibers and the matrix. This analysis was performed using a scanning electron microscope (SEM; FlexSEM 1000, Hitachi Ltd., Tokyo, Japan). Prior to observation, the specimen surfaces were sputtered with gold to ensure electrical conductivity.

Erosion performance

The trajectory of fluid particles in a rotating jet resembles a conical spiral, where each fluid particle has velocity components in three dimensions: axial velocity (u), radial velocity (v), and tangential velocity (w) (Du 2016). Given that most studies use direct jets, which lacking tangential velocity (w) for erosion wear testing. Hence, a rotating jet system was used in this study, which could accurately reflect the flow motion feature of water in natural conditions. The tests were performed using a premixed abrasive water jet device that was assembled in the laboratory (Fig. 1).

The working principle of the premixed abrasive water jet device and the test parameters were as follows. The water was pressurized to 1 MPa by a pump and was mixed with garnet particles (diameter of 149 μm) in the mixing chamber. The resulting sand-laden water stream contained 0.27 wt% garnet. This sand-laden water flowed through a pipeline into a nozzle with an inner diameter of 4 mm. Inside the nozzle, a built-in rotating impeller converted the flow into a rotating jet, which was directed at the specimen fixed on the numerical control platform. The specimens had dimensions of 50 × 50 × 5 mm³. The

shooting distances were 0.5, 1.0, and 1.5 cm, and the erosion durations were 30, 60, and 90 s. Before and after the tests, the specimens were ultrasonically cleaned at 40 kHz for 5 min and then oven-dried at 100 °C for 6 h.

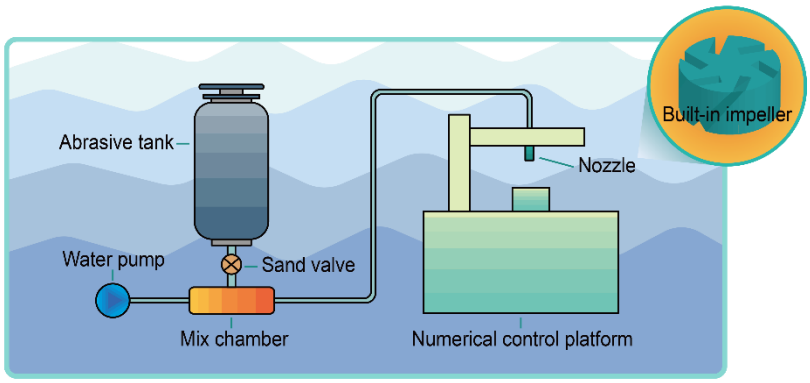

Fig. 1. Schematic drawing of premixed abrasive water jet device

The weight loss was calculated using an electronic analytical balance (FA224, LICHEN-BX Instrument Technology Co., Ltd., Shanghai, China) with an accuracy of 0.1 mg. The test results were averaged over three repetitions, and errors were eliminated through rejection and repetition of tests.

Wear mechanisms

The wear mechanisms were analyzed using a FlexSEM 1000 SEM and an energy-dispersive spectrometer (EDS; 550i, IXRF Ltd., Austin, USA), respectively. Before SEM and EDS testing, the surface to be tested was gold-sputtered to ensure electrical conductivity.

RESULTS AND DISCUSSION

Mechanical Performance

Figure 2 shows the mechanical properties of the HDPE composites. As the mass ratio of bamboo fibers to glass fibers increased, the tensile strength, breakage elongation, and impact strength of the HDPE composites tended to increase. Meanwhile, the flexural strength initially increased and then decreased slightly (by 0.86%). The maximum values of the tensile strength, breakage elongation, flexural strength, and impact strength were 8.43 MPa, 10.8%, 10.5 MPa, and 4.25 $kJ \cdot m^{-2}$, respectively, representing increases of 16.4%, 10.0%, 13.8%, and 34.9% relative to the HDPE composites without bamboo fibers.

The improvement in mechanical properties is attributed to three factors. First, compared with bamboo fibers, glass fibers have a smaller particle size and higher *L*/*D* ratio. When the filler content is excessively high, the small particle size of glass fibers will lead to agglomeration and clumping, while the large *L*/*D* ratio leads to bridging and bundling of fibers, thereby forming weak interfacial zones prone to stress accumulation. Second, bamboo fibers, which have larger particle sizes and lower *L*/*D* ratios than glass fibers, have higher surface roughness than inorganic fibers. This results in a more comprehensive structural network and a rougher surface, promoting deeper interfacial diffusion and stronger frictional interlocking with the matrix. Third, fiber reinforcement is hindered if the particle size or *L*/*D* ratio is excessively high or low. A combination of bamboo and glass fibers with different particle sizes and *L*/*D* ratios compensates for their respective drawbacks, leading to a synergistic enhancement effect (Song *et al.* 2013; Xu *et al.* 2016).

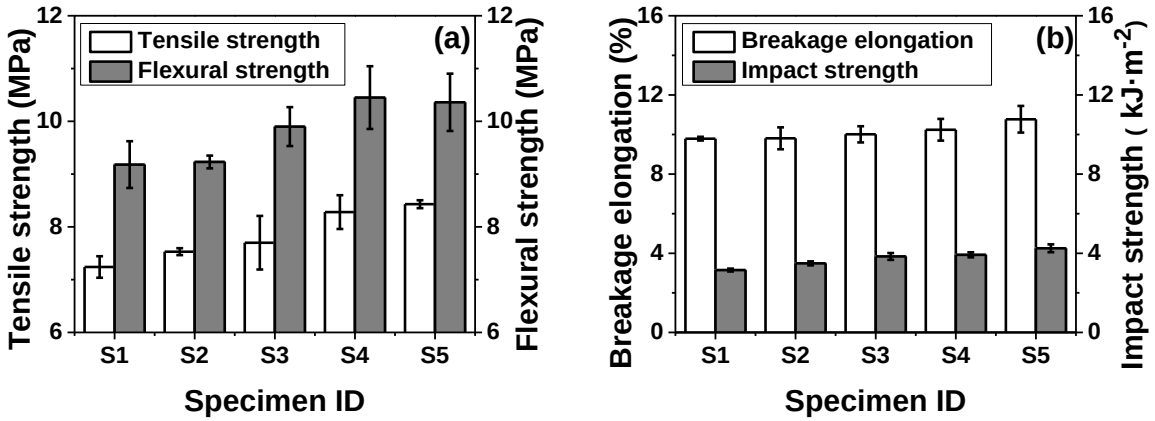

Fig. 2. Mechanical properties of the HDPE composites

Composite Structure

Figure 3 shows the FTIR spectra of the HDPE composites. A comparison between the HDPE composites with and without bamboo fibers revealed that the introduction of bamboo fibers increased the vibration amplitude in the wavenumber range of 3500 to 3300 cm^{-1} to varying degrees, while the vibration amplitudes near 2917, 2850, 1472, and 719 cm^{-1} were reduced to different degrees. This increase in the 3500 to 3300 cm^{-1} range is associated with the stretching vibration of hydroxyl (-OH) groups in cellulose, hemicellulose, polysaccharides, and monosaccharides within the bamboo fibers (Fu *et al.* 2016; Wang *et al.* 2017). It indicates that the incorporation of bamboo fibers altered the chemical structure of the HDPE composites. The increased hydroxyl content improves the hydrophilicity of the composites, reducing their resistance to water aging. Meanwhile, the reductions in vibration amplitude near 2917 and 2850 cm^{-1} are related to the asymmetric stretching vibration of the methylene (-CH_2-) groups in the matrix, and the reductions at 1472 and 719 cm^{-1} correspond to the in-plane scissoring and rocking vibrations of methylene groups, respectively (Wu *et al.* 2013). These reductions suggest the formation of chemical bonds between the bamboo fibers and the matrix.

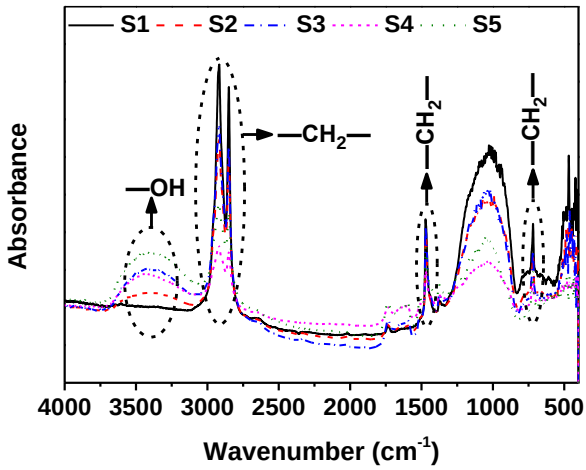

Fig. 3. FTIR spectra of the HDPE composites

Figure 4 shows the micromorphology of the tensile sections of the HDPE composites. The tensile section of the HDPE composites without bamboo fibers appeared relatively smooth, with pronounced brittle fracture characteristics. This is attributed to the difficulty in bonding the matrix with the smooth glass fibers, which hindered the frictional interlocking between the glass fibers and the matrix. In contrast, the tensile section of the HDPE composites with bamboo fibers had an uneven surface, and the brittle fracture characteristics were mitigated. This is attributed to the more intricate structural network and the rougher surface of the bamboo fibers, which allowed deeper interfacial diffusion and stronger frictional interlocking with the matrix, as discussed in the mechanical analysis section.

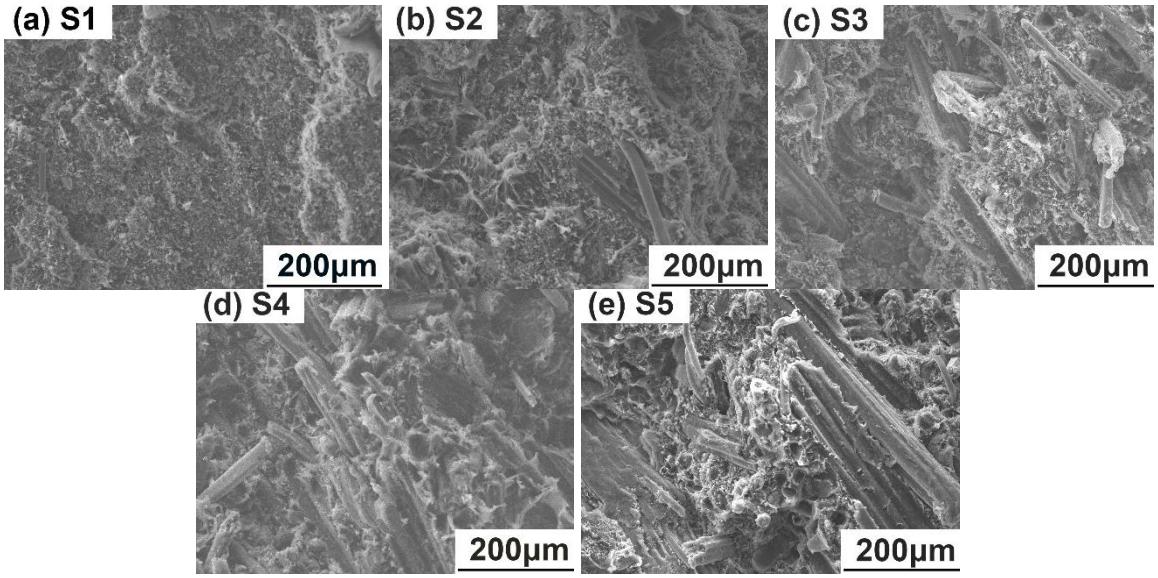

Fig. 4. Micromorphology of tensile sections of the HDPE composites

Erosion Performance

Figure 5 shows the weight loss of the HDPE composites. When the shooting distance was fixed, the weight loss of the composites increased with the erosion duration. When the erosion duration was fixed, the weight loss exhibited three trends with increasing

shooting distance: an increasing trend (specimen S1), a decreasing trend (specimens S2, S3, and S4, except for a sudden change in the case of S3 at a shooting distance of 1.5 cm and an erosion duration of 60 s), and a rise followed by a decline (specimen S5). The observed rise and fall in weight loss are attributed to the increased erosion area and reduced jet energy, respectively. The maximum weight losses for specimens S1, S2, S3, S4, and S5 were 18.85, 26.80, 25.77, 25.57, and 22.67 mg, respectively.

Figure 5 also shows that with an increasing mass ratio of bamboo fibers to glass fibers, the weight loss of the HDPE composites first increased and then decreased. The erosion resistance of the specimens decreased in the order of S1, S5, S4, S3, and S2 (except for a sudden change in the case of S3 at a shooting distance of 1.0 cm and an erosion duration of 60 s). The HDPE composites without bamboo fibers had the highest erosion resistance, indicating that replacing glass fibers with bamboo fibers reduced the erosion resistance of the composites. This is because compared with glass fibers, bamboo fibers have lower tensile, flexural, and impact strengths. Thus, the load-bearing capacity per unit area is reduced, weakening the ability to resist the embedding and plowing action of abrasive particles on the eroded surfaces. Although the erosion resistance decreased with the introduction of bamboo fibers, it tended to increase with the bamboo-to-glass fiber mass ratio. This is because the increased flexural and impact strength of the matrix allowed it to better withstand direct axial impacts from the jet, while the improved tensile strength and breakage elongation allowed the matrix to more effectively resist the tensile and shear forces generated by the radial and tangential components of the jet.

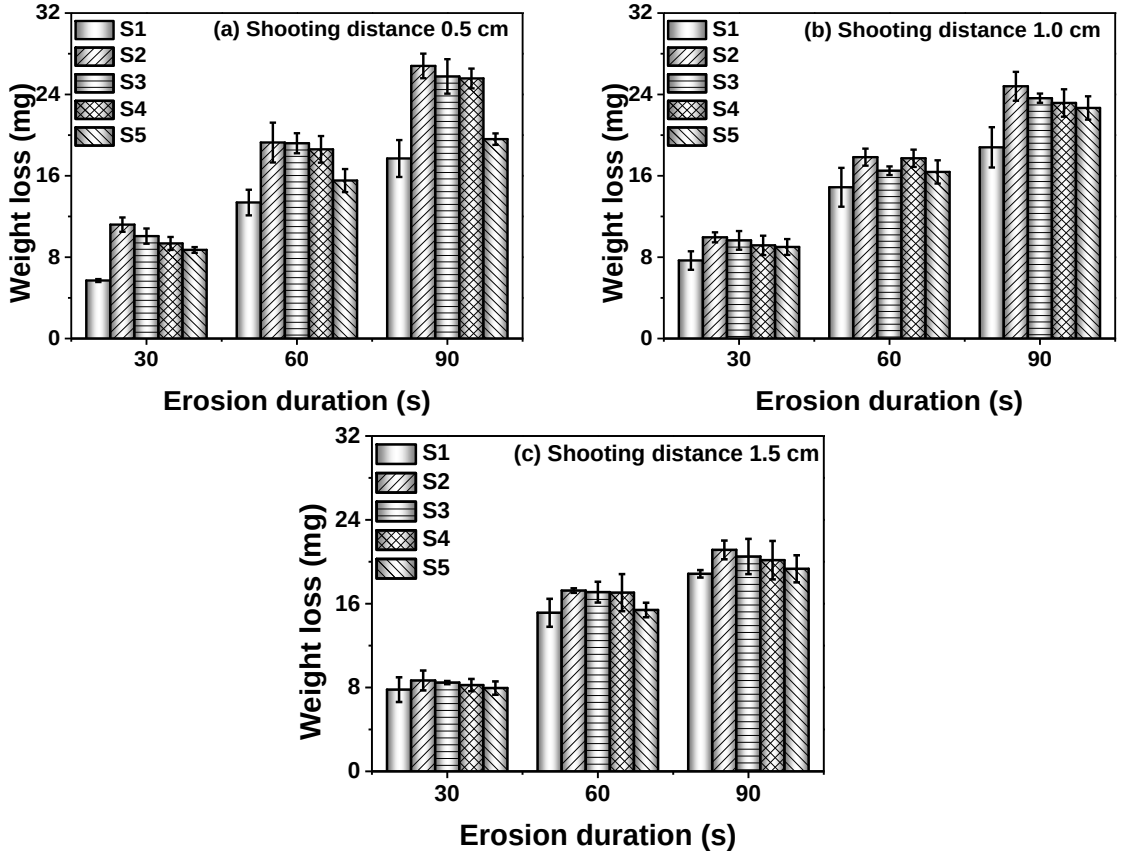

Fig. 5. Weight loss of the HDPE composites

Erosion Mechanism

Figure 6 shows the SEM images of the eroded surfaces with maximum weight loss of the HDPE composites. The HDPE composites without bamboo fibers mainly exhibited the brittle fracture characteristics of the matrix, whereas the composites with bamboo fibers exhibited both matrix brittle fracture and bamboo fiber fragmentation. In addition to the visual research of the physical morphology of the eroded surfaces, the EDS spectra of the uneroded and eroded surfaces (taken at the maximum weight loss) of the HDPE composites were investigated, as shown in Fig. 7. With an increase in the mass ratio of bamboo fibers to glass fibers, the Si content on the uneroded surfaces of the HDPE composites decreased, while the total content of C and O increased. Similarly, when the uneroded and eroded surfaces were compared, the changes in the contents of Si, C, and O followed the same trend. These results indicated that the bamboo fibers previously embedded in the matrix were extensively exposed under erosive wear conditions.

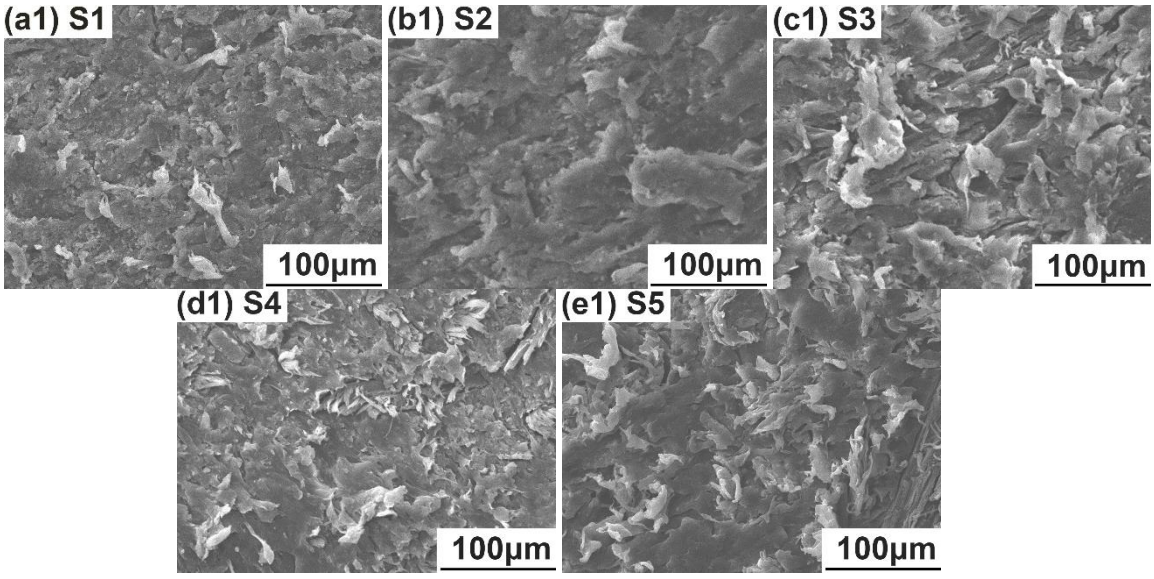

Fig. 6. SEM images of eroded surfaces with maximum weight loss of the HDPE composites

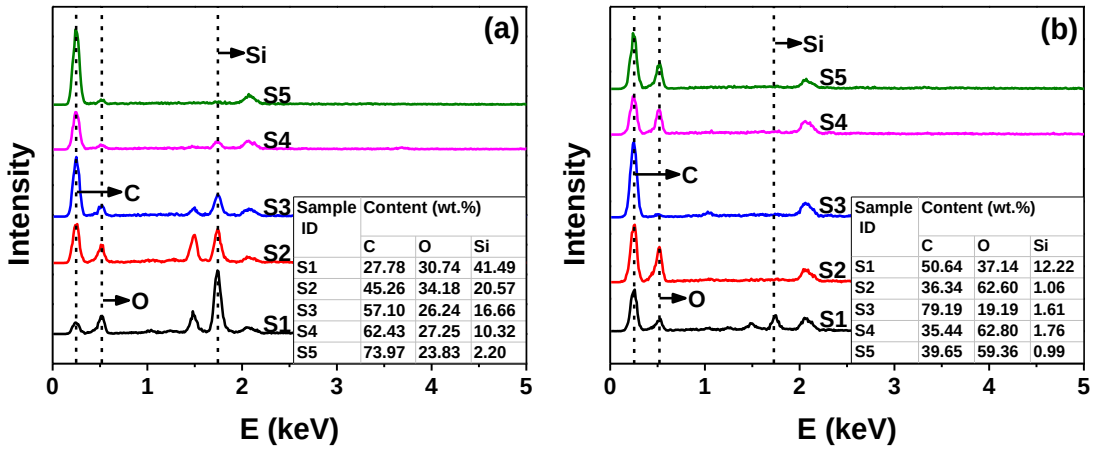

Fig. 7. EDS spectra of uneroded and eroded surfaces with maximum weight loss of the HDPE composites: (a) uneroded surfaces; (b) eroded surfaces

CONCLUSIONS

This study explores the feasibility of replacing glass fibers with bamboo fibers on the mechanical and erosive wear properties of HDPE composites. The main conclusions are as follows:

1. With an increase in the mass ratio of bamboo fibers to glass fibers, the mechanical properties of the HDPE composites generally improved, and the maximum increases in tensile strength, breakage elongation, flexural strength, and impact strength were 16.4%, 10.0%, 13.8%, and 34.9%, respectively.
2. With the increase in the mass ratio of bamboo fibers to glass fibers, the vibration amplitudes of the hydroxyl groups in the HDPE composites increased, while those of the methylene groups (asymmetric stretching, in-plane scissoring, and in-plane rocking vibrations) decreased. Bamboo fibers can chemically bond with the matrix, suppressing the brittle fracture characteristics of the tensile sections of the HDPE composites.
3. As the mass ratio of bamboo fibers to glass fibers increased, the erosion resistance of the HDPE composites initially decreased and then increased. The HDPE composites without bamboo fibers had the best erosion resistance. Erosive wear induced a brittle fracture of the matrix, bamboo fiber fragmentation, and extensive exposure of bamboo fibers on the eroded surfaces.

ACKNOWLEDGMENTS

This research was funded by the Anhui Intelligent Mine Technology and Equipment Engineering Laboratory (AIMTEEL202203) and the Study on the Aging Performance of Wood-plastic Composite Materials Used in Construction (24KJB430008).

REFERENCES CITED

Bajpai, P. K., Singh, I., and Madaan, J. (2013). "Tribological behavior of natural fiber reinforced PLA composites," *Wear* 297(1), 829-840. DOI: 10.1016/j.wear.2012.10.019

Cao, X. Y., Jia, D., Zhan, S. P., Yang, T., Li, J., and Duan, H. T. (2022). "Thermal expansion and tribological properties of glass fiber modified UHMWPE," *Polymeric Materials Science and Engineering* 38(7), 60-68. DOI: 10.16865/j.cnki.1000-7555.2022.0136

Das, G., and Biswas, S. (2017). "Erosion wear behavior of coir fiber-reinforced epoxy composites filled with Al_2O_3 filler," *Journal of Industrial Textiles* 47(4), 472-488. DOI: 10.1177/1528083716652832

Du, P. (2016). *Study on the Flow Field and Rock Breaking Mechanism of Straight-Swirling Integrated Jet*, Doctoral Dissertation, Chongqing University, Chongqing.

Fu, J. J., He, C. X., Chang, X. N., Wang, X. Z., Xiong, J., and Liu, J. H. (2016). "Thermo-stability and microstructure of wheat straw/polypropylene foamed composites," *Acta Materiae Compositae Sinica* 33(3), 469-476. DOI: 10.13801/j.cnki.fhclxb.20150615.001

Goriparthi, B. K., Suman, K. N. S., and Rao, N. M. (2012). "Effect of fiber surface

treatments on mechanical and abrasive wear performance of polylactide/jute composites," *Composites Part A: Applied Science and Manufacturing* 43(10), 1800-1808. DOI: 10.1016/j.compositesa.2012.05.007

Jenish, I., Chinnasamy, S. G. V., Basavarajappa, S., Indran, S., Divya, D., Liu, Y. C., Sanjay, M. R., and Siengchin, S. (2022). "Tribo-Mechanical characterization of carbonized coconut shell micro particle reinforced with Cissus quadrangularis stem fiber/epoxy novel composite for structural application," *Journal of Natural Fibers* 19(8), 2963-2979. DOI: 10.1080/15440478.2020.1838988

Jeamtrakull, S., Kositchaiyong, A., Markpin, T., Rosarpitak, V., and Sombatsompop, N. (2012). "Effects of wood constituents and content, and glass fiber reinforcement on wear behavior of wood/PVC composites," *Composites Part B: Engineering* 43(7), 2721-2729. DOI: 10.1016/j.compositesb.2012.04.031

Jiang, L. P., Yang, Y., Fu, J. J., Teng, W. X., and Wang, H. (2022a). "Erosive wear analysis of bamboo fiber-reinforced high-density polyethylene composites: Effect of aluminum oxide," *Polymer Composites* 43(6), 3823-3830. DOI: 10.1002/pc.26658

Jiang, L. P., Wan, Y. T., Zhang, N., Fu, J. J., Li, X. K., Zhang, X. W., and Du, P. (2022b). "Erosive wear characteristics of styrene butadiene rubber and silicon dioxide-filled wood–plastic composites," *Journal of Building Engineering* 56, 104791. DOI: 10.1016/j.jobe.2022.104791

Kunishima, T., Nagai, Y., Kurokawa, T., Bouvard, G., Abry, J., Fridrici, V., and Kapsa, P. (2020). "Tribological behavior of glass fiber reinforced-PA66 in contact with carbon steel under high contact pressure, sliding and grease lubricated conditions," *Wear* 456, 203383. DOI: 10.1016/j.wear.2020.203383

Kalusuraman, G., Kumaran, T. S., Aslan, M., Küçükömeroğluc, T., and Siva, I. (2019). "Use of waste copper slag filled jute fiber reinforced composites for effective erosion prevention," *Measurement* 148, 106950. DOI: 10.1016/j.measurement.2019.106950

Li, X. K., Fu, J. J., and Jiang, L. P. (2022). "Erosion wear behavior of bamboo fiber-reinforced high-density polyethylene composites with nano silicon dioxide filler subjected to rotary water jet," *BioResources* 17(3), 5178-5189. DOI: 10.15376/biores.17.3.5178-5189

Palanisamy, S., Ramakrishnan, S. K., Santulli, C., Khan, T., and Ahmed, O. S. (2024). "Mechanical and wear performance evaluation of natural fiber/epoxy matrix composites," *BioResources* 19(4), 8459-8478. DOI: 10.15376/biores.19.4.8459-8478

Qi, R. G., He, C. X., Fu, J. J., Zhao, L. M., and Jiang, C. Y. (2019). "Effect of inorganic nanoparticles on the thermal and mechanical properties of wood fiber/HDPE composites," *Journal of Shanghai Jiaotong University* 53(3), 373-379. DOI: 10.16183/j.cnki.jsjtu.2019.03.016

Ramakrishnan, S. K., Vijayananth, K., Arivendan, A., and Ammarullah, M. I. (2024). "Evaluating the effects of pineapple fiber, potato waste filler, surface treatment, and fiber length on the mechanical properties of polyethylene composites for biomedical applications," *Results in Engineering* 24, 102974. DOI: 10.1016/j.rineng.2024.102974

Rangappa, S. M., Parameswaranpillai, J., Siengchin, S., Jawaid, M., and Ozbakkaloglu, T. (2022). "Bioepoxy based hybrid composites from nano-fillers of chicken feather and lignocellulose Ceiba Pentandra," *Scientific reports* 12(1), 397. DOI: 10.1038/s41598-021-04386-2

Song, L. X., Zhang, P., Yao, N. N., Song, Y. Z., Kang, M., and Song, K. P. (2013). "Study on effect of particle diameter and filling quantity of wood flour on mechanical

properties of wood-plastics composite," *Journal of Functional Materials* 44(17), 2451-2454. DOI: 10.3969/j.issn.1001-9731.2013.17.003

Vigneshwaran, S., Uthayakumar, M., and Arumugaprabu, V. (2019). "Solid particle erosion study on redmud - An industrial waste reinforced sisal/polyester hybrid composite," *Materials Research Express* 6(6), 065307. DOI: 10.1088/2053-1591/ab0a44

Wang, B. W., Yu, S. D., Mao, J., Wang, Y. H., Li, M. J., and Li, X. P. (2021). "Effect of basalt fiber on tribological and mechanical properties of polyether-ether-ketone (PEEK) composites," *Composite Structures* 266, 113847. DOI: 10.1016/j.compstruct.2021.113847

Wang, M., He, C. X., Zhu, G. L., and Zhang, J. (2017). "Performance comparison of different plant fibers/bone glue composites," *Acta Materiae Compositae Sinica* 34(5), 1103-1110. DOI: 10.13801/j.cnki.fhclxb.20160825.004

Wu, Q. N., Yang, W. B., Yu, F. B., and Chen, L. H. (2013). "Effect of hydrothermal treatment on properties of reversibly thermochromic bamboo/plastic composite," *Acta Materiae Compositae Sinica* 30(6), 28-36. DOI: 10.13801/j.cnki.fhclxb.2013.06.013

Xu, J. J., Hao, X. L., Zhou, H. Y., Sun, L. C., Liu, T., Wang, Q. W., and Ou, R. X. (2021). "High- and low-temperature performance of ultra-highly filled polypropylene-based wood plastic composite," *Acta Materiae Compositae Sinica* 38(12), 4106-4122. DOI: 10.13801/j.cnki.fhclxb.20210317.002

Xu, H. L., Cao, Y., Wang, W. H., Wang, Q. W., and Wang, H. G. (2016). "Effects of poplar wood fiber size on mechanical and creep properties of poplar wood fiber/high-density polyethylene composites prepared by hot-compression molding," *Acta Materiae Compositae Sinica* 33(6), 1168-1173. DOI: 10.13801/j.cnki.fhclxb.20160107.003

Zhang, J., Ning, L. P., Yang, H. J., Wu, B. L., Luo, S., and Rong, Z. L. (2016). "Effects of glass fiber content on properties of bamboo flour/high density polyethylene composites," *Acta Materiae Compositae Sinica* 33(3), 477-485. DOI: 10.13801/j.cnki.fhclxb.20150623.004

Zhang, L., Sun, J. P., Yu, Q. Y., Li, R. Y., Zhang, Y. H., and Wang, W. J. (2020). "Effect of hydrophobic modification of wood flour on properties of HDPE based wood plastic composites," *Chemical Industry and Engineering Progress* 39(9), 3487-3493. DOI: 10.16085/j.issn.1000-6613.2019-1873

Article submitted: November 29, 2024; Peer review completed: February 5, 2025;
Revisions accepted: March 13, 2025; Published: April 10, 2025.
DOI: 10.15376/biores.20.2.4033-4043